Structures and adsorption of binary hard-core Yukawa mixtures in a slitlike pore: Grand canonical Monte Carlo simulation and density-functional study

Feng-Qi You, Yang-Xin Yu,[a] and Guang-Hua Gao
Department of Chemical Engineering, Tsinghua University, Beijing 10084, People's Republic of China and State Key Laboratory of Chemical Engineering, Tsinghua University, Beijing 100084, People's Republic of China

(Received 4 May 2005; accepted 11 July 2005; published online 19 September 2005)

The grand canonical ensemble Monte Carlo simulation and density-functional theory are applied to calculate the structures, local mole fractions, and adsorption isotherms of binary hard-core Yukawa mixtures in a slitlike pore as well as the radial distribution functions of bulk mixtures. The excess Helmholtz energy functional is a combination of the modified fundamental measure theory of Yu and Wu [J. Chem. Phys. **117**, 10156 (2002)] for the hard-core contribution and a corrected mean-field theory for the attractive contribution. A comparison of the theoretical results with the results from the Monte Carlo simulations shows that the corrected theory improves the density profiles of binary hard-core Yukawa mixtures in the vicinity of contact over the original mean-field theory. Both the present corrected theory and the simulations suggest that depletion and desorption occur at low temperature, and the local segregation can be observed in most cases. For binary mixtures in the hard slitlike pore, the present corrected theory predicts more accurate surface excesses than the original one does, while in the case of the attractive pore, no improvement is found in the prediction of a surface excess of the smaller molecule. © *2005 American Institute of Physics*. [DOI: 10.1063/1.2013247]

I. INTRODUCTION

Recently, a close-packed monodisperse silica or latex nanoparticle has been proposed for application in microphotonic crystal devices and chips.[1] Understanding the fundamental mechanisms that drive the assembly of particles at microscopic level will bring about new strategies for the fabrication of well-ordered arrays of nanoscale objects. On the other hand, the structure of colloids in confining geometry is closely related to this self-assembly of colloidal particles for material applications. Since the interaction between colloidal particles is well described by a hard-core Yukawa (HCY) potential,[2,3] an investigation on the static density distribution of the HCY fluids provides a useful starting point for understanding the self-assembly of colloidal particles and the microscopic flow behavior.

A lot of researches have been carried out to investigate the pair-correlation functions, phase equilibria, thermodynamic properties, and surface tensions of the pure HCY fluids using integral equation theory, perturbation theory, and Monte Carlo simulations,[4–12] while few works have been done on the HCY fluid mixtures.[13,14] As for the inhomogeneous HCY fluids, all the studies are limited to the pure attractive and repulsive HCY fluids. For example, Olivares-Rivas *et al.*[15] used the singlet hypernetted-chain integral equation and a modified version of the Lovett-Mou-Buff-Wertheim equation to predict the density profiles near a hard wall at reduced density $\rho_b\sigma^3=0.7$. Several versions[16–19] of density-functional theory (DFT) are also developed for the pure HCY fluid confined in a pore or near a wall. Among these versions of DFT, our method[19] and the one proposed by Tang,[18] both of which are based on the modified fundamental measure theory (MFMT)[20–22] for the hard-core contribution and Rosenfeld's perturbative expansion,[19,23–27] are the most promising theories for inhomogeneous HCY fluids. However, no investigation on confined HCY fluid mixtures is reported up to now.

In our previous work,[20,28] we applied the grand canonical ensemble Monte Carlo (MC) simulation and the DFT to the investigation of the structures of attractive and repulsive HCY fluids near a wall as well as the radial distribution functions of the bulk HCY fluids. An excellent agreement between theory and simulation is obtained. In this work, we continue our investigation on the inhomogeneous HCY fluids and focus on the binary systems using the MC simulation and the DFT. The key problem of the DFT is that we have to find a good approximation of the excess Helmholtz energy functional. The DFT has enjoyed some remarkable successes for hard-sphere fluids.[21] In particular, the MFMT yields very accurate density profiles for inhomogeneous hard-sphere fluids[23] and is easily applied to multicomponent and polydisperse hard-sphere fluids.[27,29,30] In contrast, the DFTs for the dispersion force are only satisfactory in the case of one-component system. Since there is no analytical expression of the direct correlation functions for the HCY fluid mixture, it is difficult to use Rosenfeld's perturbative method[31] to construct the excess Helmholtz energy functional of binary HCY fluid mixtures. An alternative way is to use the popular

[a]Author to whom correspondence should be addressed. Electronic mail: yangxyu@mail.tsinghua.edu.cn

mean-field (MF) theory,[18,19] which is simple, computationally efficient, and can be directly applied to multicomponent systems. The shortcomings of the MF theory are apparent. It neglects the fluid structure completely, and its performance is highly system dependent.[32,33] It usually overestimates the density at a hard surface and gives too strong oscillations of density profiles.[34,35] It is reduced to the well-known van der Waals equation of state at the homogeneous limit. Some modifications[36] have been made to improve the MF theory, but they are semiempirical and do not solve the fundamental problems in the MF theory. A recent modification[19] of the MF theory adopts the so-called effective reference field and successfully addresses the interfacial and hydrophobic phenomena in inhomogeneous fluids.[20,21] In this work, the Helmholtz energy functional of the HCY fluid mixtures are constructed by combining the MFMT for the hard-core interaction with the MF theory for the Yukawa dispersion interaction. To cover the shortage of the MF theory, we introduce a constant c to "correct" the MF theory just as we make a correction of energy parameter a in the van der Waals equation of state. The constant c is determined from the bulk chemical potential of pure HCY fluids. Then the theory is applied to investigating the density profiles and surface excesses of binary Yukawa fluid mixtures in a slitlike pore as well as the radial distribution functions of bulk binary HCY fluid mixtures. To test the prediction of the present DFT, the grand canonical ensemble Monte Carlo (GCMC) simulations have been carried out to obtain the density profiles of binary HCY fluid mixtures in a slitlike pore under different temperatures, energy parameter and diameter ratios, and bulk mole fractions and densities.

In what follows, we present the DFT theory for binary HCY fluid mixtures in Sec. II, the Monte Carlo method in Sec. III, the numerical results for the density profiles, the radial distribution functions, and the surface excesses in Sec. IV, and a few general conclusions in Sec. V.

II. THEORY

A. Model

We consider an N-component mixture of hard-core Yukawa fluid. The pairwise-additive two-body potential is given by

$$u_{ij}(r) = \begin{cases} \infty & r < \sigma_{ij} \\ -\dfrac{\varepsilon_{ij}\sigma_{ij}\exp[-\lambda(r-\sigma_{ij})/\sigma_{ij}]}{r}, & r > \sigma_{ij}, \end{cases} \tag{1}$$

where $\sigma_{ij}=(\sigma_i+\sigma_j)/2$, $\varepsilon_{ij}=(\varepsilon_i\varepsilon_j)^{1/2}$, σ_i is the diameter of species i, ε_i is the energy parameter, r is the center-to-center distance between two interacting Yukawa spheres, and λ is the screening length for the Yukawa tail. Throughout this work, the hard-sphere Yukawa potential with the range parameter $\lambda=1.8$ is used. We investigate the structures and surface excesses for binary HCY fluid mixtures confined in a slit pore under different conditions using the density-functional theory and Monte Carlo simulations.

B. Density-functional theory

The essential task for a density-functional theory is to derive an analytical expression for the grand potential Ω, or equivalently, the intrinsic Helmholtz free-energy F, as a functional of density distribution $\rho_i(\mathbf{r})$. For an N-component fluid mixture at given temperature T, total volume V, chemical potential μ_i, and external potential $V_i^{\mathrm{ext}}(\mathbf{r})$ for each component, the grand potential is minimized at equilibrium and the equilibrium density distribution $\rho_i(\mathbf{r})$ satisfies

$$\delta\Omega[\rho_i(\mathbf{r})]/\delta\rho_i(\mathbf{r}') = 0 \quad (i = 1,2,\ldots,N). \tag{2}$$

The grand potential for an inhomogeneous HCY fluid mixture is related to the Helmholtz energy functional through the Legendre transform,

$$\Omega[\rho_i(\mathbf{r})] = F[\rho_i(\mathbf{r})] + \sum_{i=1}^{N} \int d\mathbf{r}\rho_i(\mathbf{r})[V_i^{\mathrm{ext}}(\mathbf{r}) - \mu_i]. \tag{3}$$

Once we have an expression for the intrinsic Helmholtz free-energy functional, the solution to Eq. (2) gives the equilibrium density profiles and, subsequently, the relevant thermodynamic properties.

To take into account the nonideality arising from intermolecular interactions, the intrinsic Helmholtz free-energy functional is often expressed as contribution from an ideal-gas term and an excess term due to intermolecular interactions:

$$F = F^{\mathrm{id}} + F^{\mathrm{ex}}, \tag{4}$$

where the ideal intrinsic Helmholtz free-energy functional F^{id} is known exactly,

$$F^{\mathrm{id}} = k_B T \sum_{i=1}^{N} \int d\mathbf{r}[\ln(\rho_i(\mathbf{r})\Lambda_i^3) - 1]\rho_i(\mathbf{r}), \tag{5}$$

where k_B is the Boltzmann constant, T is the absolute temperature, and $\Lambda_i = h/(2\pi m_i k_B T)^{1/2}$ is the thermal de Broglie wavelength.

The central topic of a density-functional theory is to derive an analytical expression for the excess Helmholtz free energy as a functional of the density distributions. The excess Helmholtz free-energy functional can be further decomposed into the contributions from the hard-sphere repulsion and long-ranged attraction:

$$F^{\mathrm{ex}} = F_{\mathrm{hs}}^{\mathrm{ex}} + F_{\mathrm{att}}^{\mathrm{ex}}. \tag{6}$$

As in the previous work,[20,37] we apply the MFMT[38] for the functional $F_{\mathrm{hs}}^{\mathrm{ex}}$ in Eq. (6). The mathematical expression of the excess Helmholtz free-energy functional in the MFMT is given by

$$F_{\mathrm{hs}}^{\mathrm{ex}} = k_B T \int \Phi^{\mathrm{hs}}[n_\alpha(\mathbf{r})]d\mathbf{r}, \tag{7}$$

where $\Phi^{\mathrm{hs}}[n_\alpha(\mathbf{r})]$ is the reduced excess Helmholtz free-energy density due to the hard-sphere repulsion and $n_\alpha(\mathbf{r})$ is the weighted density. The weighted densities can be expressed as

$$n_\alpha(\mathbf{r}) = \sum_{i=1}^{N} n_{\alpha,i}(\mathbf{r}) = \sum_{i=1}^{N} \int \rho_i(\mathbf{r}') w_i^{(\alpha)}(|\mathbf{r}-\mathbf{r}'|) d\mathbf{r}', \tag{8}$$

where the subscripts $\alpha=0$, 1, 2, 3, $V1$, and $V2$ denote the index of six weight functions $w_i^{(\alpha)}(r)$. The six weight functions can be found in our previous work[20,21] and in the paper of Boublik[39] and Mansoori *et al.*[40] In the MFMT, the excess Helmholtz free-energy density due to the hard-sphere repulsion consists of contributions from the scalar-weighted densities and the vector-weighted densities,[41–44]

$$\Phi^{\mathrm{hs}}[n_\alpha(\mathbf{r})] = \Phi^{\mathrm{hs}(S)}[n_\alpha(\mathbf{r})] + \Phi^{\mathrm{hs}(V)}[n_\alpha(\mathbf{r})], \tag{9}$$

where the superscripts (S) and (V) stand for the contributions from scalar- and vector-weighted densities, respectively. The scalar Helmholtz energy density is given by

$$\Phi^{\mathrm{hs}(S)}[n_\alpha(\mathbf{r})] = -n_0 \ln(1-n_3) + \frac{n_1 n_2}{1-n_3} + \frac{n_2^3 \ln(1-n_3)}{36\pi n_3^2} + \frac{n_2^3}{36\pi n_3 (1-n_3)^2}, \tag{10}$$

and the vector part is expressed by

$$\Phi^{\mathrm{hs}(V)}[n_\alpha(\mathbf{r})] = -\frac{\mathbf{n}_{V1}\cdot\mathbf{n}_{V2}}{1-n_3} - \frac{n_2 \mathbf{n}_{V2}\cdot\mathbf{n}_{V2} \ln(1-n_3)}{12\pi n_3^2} - \frac{n_2 \mathbf{n}_{V2}\cdot\mathbf{n}_{V2}}{12\pi n_3 (1-n_3)^2}. \tag{11}$$

In the limit of a bulk fluid, the two vector-weighted densities $\mathbf{n}_{V1}$ and $\mathbf{n}_{V2}$ vanish, and the excess Helmholtz energy density Φ^{hs} becomes identical to that from the Boublik-Mansoori-Carnahan-Starling-Leland (BMCSL) equation of state.[19]

To obtain the attractive part of the Helmholtz free-energy functional, one may perform a quadratic functional Taylor expansion around the bulk fluid, as what have been done for the restricted-primitive-model electrolyte solutions[39,40] and pure hard-core Yukawa fluid.[39,40] In this method, the second-order direct correlation function is required. However, to our knowledge there is no analytical expression of the second-order direct correlation function for the binary hard-core Yukawa fluid mixture. Alternatively, the attractive part of the Helmholtz free-energy functional can be expressed as

$$F_{\mathrm{att}}^{\mathrm{ex}}[\rho(\mathbf{r})] = \frac{1}{2}\sum_{i=1}^{N}\sum_{j=1}^{N} \int\int d\mathbf{r} d\mathbf{r}' \rho_i(\mathbf{r}) \rho_j(\mathbf{r}') \times g_{ij}(\mathbf{r},\mathbf{r}') u_{ij}(|\mathbf{r}-\mathbf{r}'|), \tag{12}$$

where $g_{ij}(\mathbf{r},\mathbf{r}')$ is the radial distribution function (RDF) between spheres i and j for the inhomogeneous fluid. Generally, it is difficult to be obtained and when we set $g_{ij}(\mathbf{r},\mathbf{r}')=1$, the most popular method for the dispersion force—the mean-field (MF) theory—is reproduced.

$$F_{\mathrm{att}}^{\mathrm{ex}}[\rho(\mathbf{r})] = \frac{1}{2}\sum_{i=1}^{N}\sum_{j=1}^{N} \int\int d\mathbf{r} d\mathbf{r}' \rho_i(\mathbf{r}) \rho_j(\mathbf{r}') u_{ij}(|\mathbf{r}-\mathbf{r}'|). \tag{13}$$

Apart from its simplicity in form and its computational efficiency, the MF theory often overestimates the contact values of density and the oscillations of density profiles due to its complete neglect of the fluid structure. In this work, we introduce a constant c to correct the attractive part of the excess Helmholtz free-energy functional, where c is related to the fluid properties just as a correction of the parameter a in the famous van der Waals equation of state. From the comparison of the simulated chemical potentials for pure hard-core Yukawa fluid with the chemical potential of hard spheres from BMCSL equation of state,[45] we can obtain the value of parameter c in different conditions. Then the attractive part of the Helmholtz free-energy functional can be expressed as

$$F_{\mathrm{att}}^{\mathrm{ex}}[\rho(\mathbf{r})] = \frac{c}{2}\sum_{i=1}^{N}\sum_{j=1}^{N} \int\int d\mathbf{r} d\mathbf{r}' \rho_i(\mathbf{r}) \rho_j(\mathbf{r}') u_{ij}(|\mathbf{r}-\mathbf{r}'|). \tag{14}$$

At the equilibrium, the grand potential $\mathbf{\Omega}[\rho_i(\mathbf{r})]$ reaches its minimum. From Eq. (2), we can obtain the following Euler-Lagrange equation for the density profile

$$\rho_i(\mathbf{r}) = \rho_i^b \exp\left\{ \beta\mu_i^{\mathrm{ex}} - \int d\mathbf{r}' \left[\sum_\alpha \frac{\partial \Phi^{\mathrm{hs}}}{\partial n_\alpha(\mathbf{r})} w_i^{(\alpha)}(|\mathbf{r}'-\mathbf{r}|) \right] - \beta V_i^{\mathrm{ext}}(\mathbf{r}) - c\beta \sum_{j=1}^{N} \int d\mathbf{r}' \rho_j(\mathbf{r}') u_{ij}(|\mathbf{r}-\mathbf{r}'|) \right\}, \tag{15}$$

where $F_{\mathrm{hs}}^{\mathrm{ex}}$ is evaluated from Eq. (7), ρ_i^b is the bulk density of component i, and μ_i^{ex} is the excess chemical potential of component i, i.e.,

$$\mu_i^{\mathrm{ex}} = \mu_{i,\mathrm{hs}}^{\mathrm{ex}} + c\mu_{i,\mathrm{MF}}^{\mathrm{ex}}, \tag{16}$$

where $\mu_{i,\mathrm{hs}}^{\mathrm{ex}}$ is the excess chemical potential due to the hard-sphere repulsion, which can be obtained from the BMCSL equation of state,[19] and $\mu_{i,\mathrm{MF}}^{\mathrm{ex}}$ is obtained by the functional derivative of Eq. (13) with respect to the density distribution in the bulk limit. Let us call this density-functional theory as MFMT-cMF theory; when $c=1$, it is reduced to the mean-field (MFMT-MF) theory.

When the HCY fluid mixture is confined in a slit pore or around a fixed spherical particle, the density profiles only vary in the z direction or r direction, i.e., $\rho_i(\mathbf{r})=\rho_i(z)$ or $\rho_i(\mathbf{r})=\rho_i(r)$. The density profiles are solved from Eq. (15) using the Picard-type iterative method. The iteration starts with the corresponding bulk density as an initial guess. The next input is obtained by mixing the new density profile with the previous one. The numerical integrations are performed using the trapezoidal rule with the step size Δz or $\Delta r = 0.005\sigma$, and the iteration is repeated until the percentage change is smaller than 10^{-4} at all points.

III. MONTE CARLO SIMULATIONS

In order to test the validity of the DFT, the GCMC simulations are carried out in this work for binary HCY fluid mixtures at different temperatures, bulk densities, mole frac-

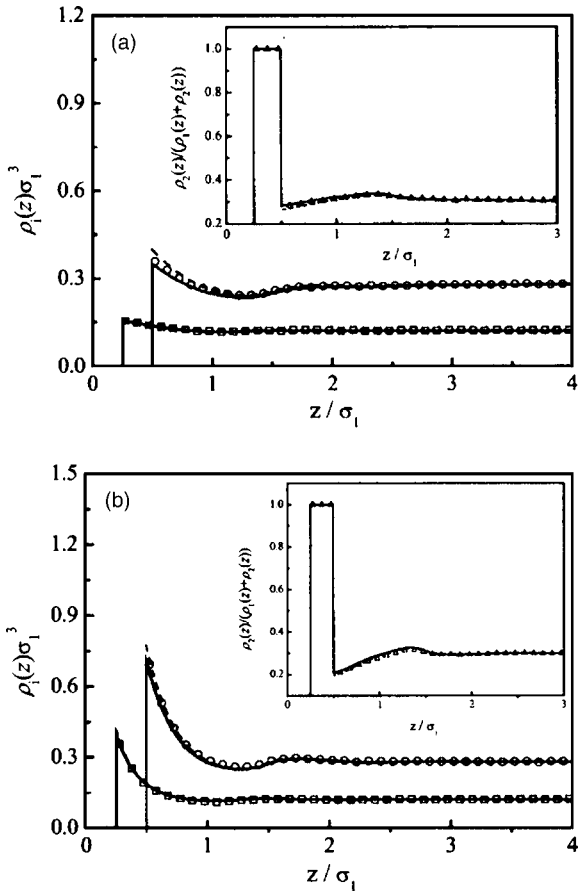

FIG. 1. Density and local concentration (inset) profiles of a binary HCY mixture in a slitlike pore (pore with $H=10\sigma$) at the diameter ratio $\sigma_2/\sigma_1=0.5$, reduced temperature $T^*=3.0$, energy parameter ratio $\varepsilon_2/\varepsilon_1=0.5$, bulk mole fraction $x_1^b=0.7$, reduced bulk density $\rho_b\sigma_1^3=0.4$, and energy parameters of wall: (a) $\varepsilon_W/k_BT=0$ and (b) $\varepsilon_W/k_BT=1.0$. The symbols, dashed curves, and solid curves represent the results from the GCMC simulation, MFMT-MF, and MFMT-*c*MF theories, respectively.

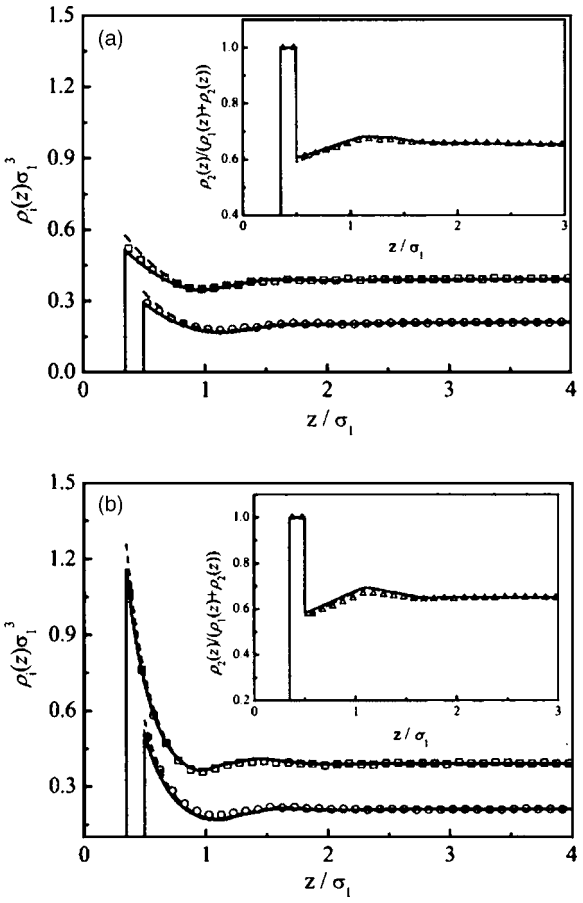

FIG. 2. Same as in Fig. 1 but at the diameter ratio $\sigma_2/\sigma_1=0.7$, energy parameter ratio $\varepsilon_2/\varepsilon_1=1.0$, bulk mole fraction $x_1^b=0.35$, and reduced density $\rho_b\sigma_1^3=0.6$.

tions, energy parameters, and diameter ratios. Before the GCMC simulations, Wisdom's tets-particle method in an *NVT* ensemble is used to determine the excess chemical potential of each component in the binary mixtures under the considered conditions. The conventional Metropolis algorithm is used for generating successive configurations with the probability of a successful displacement adjusted to 50% of all particles. At each calculation, the simulation box contains 1000 particles, in which two kinds of Yukawa molecules are distributed according to the composition. At each condition, about 9×10^5 complete MC cycles are run for sampling after 1×10^5 MC cycles are run for equilibration. In each MC sampling cycle, all particles are displaced once, and then each of the two kinds of test Yukawa molecules are inserted into the system five times to obtain excess chemical potentials of the two components because this may enable the phase space to be covered more efficiently if an appropriate value for the maximum displacement is chosen. Meanwhile, the standard method was used to obtain the radial distribution functions of the binary HCY mixtures.

The GCMC simulation is then carried out with the excess chemical potentials obtained above. The mixture fluids are confined between the two parallel walls with pore width $H=10\sigma_1$. The simulation box is cubic $(10\sigma_1\times10\sigma_1\times10\sigma_1)$, and the particles are originally placed as an fcc configuration. Four different types of move, including displacement, particle creation, particle deletion, and exchange of the two kinds of particles are performed with a ratio of 3:1:1:1. The inserted particles in the system are chosen with a ratio corresponding to the mole fraction of the bulk binary mixtures. The usual periodic boundary conditions and minimum image conventions are applied in the directions parallel to the walls. The cutoff distance of Yukawa potential is set to $5\sigma_1$. Beyond this distance, the Yukawa potential is small enough that the Ewald sum can be neglected. At each condition, about 1×10^8 complete MC cycles are run for equilibration, and then another 9×10^8 MC cycles are run for sampling the density distributions of the two components. The density profile is recorded by dividing the region between the walls into a number of equal-sized bins. It is obtained by averaging the number of each type of spheres in the bin during the period of the run for sampling.

IV. RESULTS AND DISCUSSIONS

A. Binary Yukawa fluid mixtures in a slitlike pore

To obtain density profiles from Eq. (15), we need to determine constant c at first. The correction parameter c is just like the correction to parameter a in the famous van der Waals equation. We determine constant c from the simulated

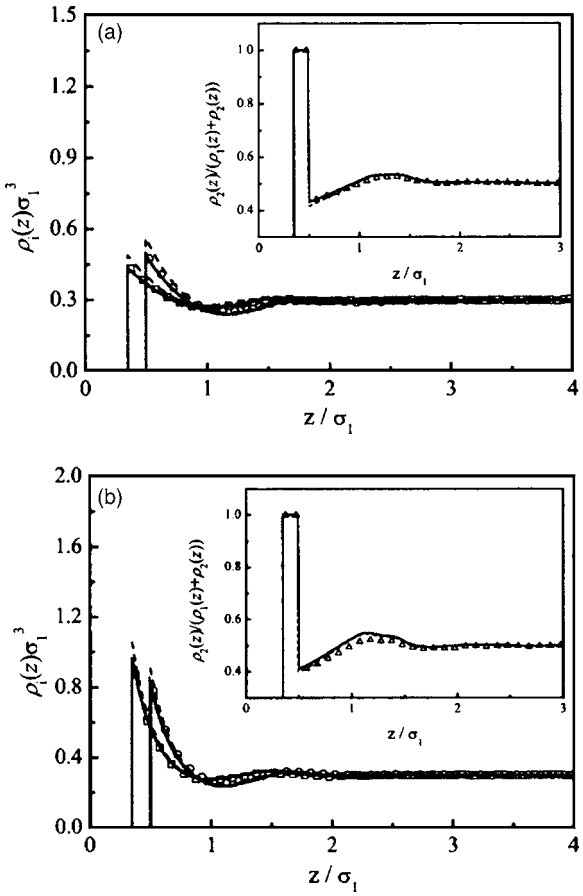

FIG. 3. Same as in Fig. 1 but at the diameter ratio $\sigma_2/\sigma_1=0.7$, energy parameter ratio $\varepsilon_2/\varepsilon_1=1.0$, bulk mole fraction $x_1^b=0.5$, and reduced density $\rho_b\sigma_1^3=0.6$.

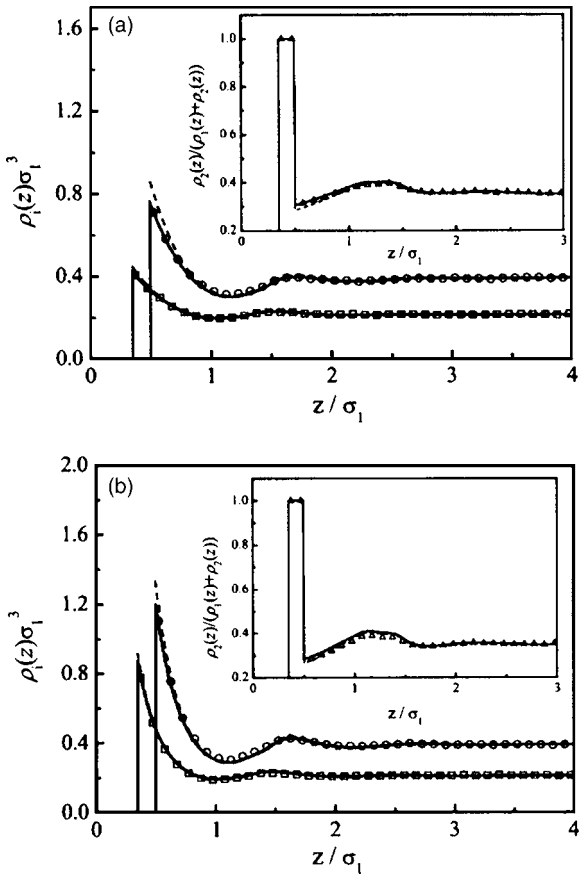

FIG. 4. Same as in Fig. 1 but at the diameter ratio $\sigma_2/\sigma_1=0.7$, energy parameter ratio $\varepsilon_2/\varepsilon_1=0.5$, bulk mole fraction $x_1^b=0.65$, and reduced density $\rho_b\sigma_1^3=0.6$.

chemical potentials of pure Yukawa fluid according to Eq. (16). The excess chemical potential is determined using Widom's test-particle method for the pure HCY fluid with $\lambda=1.8$ under different temperatures and densities. From the simulated chemical potentials we find that parameter c is independent of temperature and varies slightly with reduced density. When the density tends to zero, the constant c should be a unit. However constant c at low density has little effect on the density profiles near a wall. Furthermore, if we assume that c is constant at any reduced densities and temperatures, the simple expression of the Helmholtz free-energy functional can be easily obtained. Otherwise, we need a set of constants "c_{ij}" specific to each of the different interactions between particles of species i and j. For convenience, we keep $c=1.31$ at any reduced densities and temperatures throughout this work. It should be pointed out that the constant $c=1.31$ is obtained from the simulated chemical potential data of pure Yukawa fluid at reduced density $\rho_b\sigma_1^3=0.6$ and various temperatures.

Now we discuss the density profiles of the binary HCY fluid mixtures in a slitlike pore under various conditions. The external potential from the parallel walls can be expressed as

$$V_i^{\mathrm{ext}}(z)=\begin{cases} W_i(z)+W_i(H-z), & \sigma_i/2 \leqslant z \leqslant H-\sigma_i/2 \\ \infty, & \text{otherwise,} \end{cases} \tag{17}$$

where

$$W_i(z)=-\varepsilon_W \exp\{-\lambda(z-\sigma_i/2)/\sigma_i\}, \tag{18}$$

where ε_W is the energy parameter of the wall and z is the perpendicular distance from the left wall. H is the width of the slitlike pore. Throughout this work the width of the pore is $H=10\sigma_1$. The bulk conditions used in the calculations are specified by the reduced temperature $T^*=k_BT/\varepsilon_1$, hard-core diameter ratio σ_2/σ_1, energy parameter ratio $\varepsilon_2/\varepsilon_1$, bulk mole fraction x_i^b, and reduced bulk density $\rho_b\sigma_1^3$, where ρ_b is the total number density of the bulk fluid, i.e., $\rho_b=\Sigma_{i=1}^N\rho_i^b$. In all the calculations in this work, σ_1 is selected as the unit length.

In Figs. 1(a) and 1(b), we compare the calculated density and local mole fraction (inset) profiles in a slitlike pore with those of the GCMC simulations for a binary HCY mixture at $T^*=3.0$, $\sigma_2/\sigma_1=0.5$, $\varepsilon_2/\varepsilon_1=0.5$, $x_1^b=0.7$, and $\rho_b\sigma_1^3=0.4$. In all the cases of the binary HCY mixtures confined in the slit pore, two wall energy parameters $\varepsilon_w/k_BT=0$ and 1.0 are considered. Just as in a pure HCY fluid, the density profiles and the mole fraction profiles occur with less oscillation near a hard wall at this low bulk density. When the wall has an attractive force [see Fig. 1(b)], there is an accumulation of the HCY fluids near the wall, and surface segregation occurs. It can be seen from Fig. 1 that the MFMT-cMF theory accurately predicts the density and mole fraction profiles. The

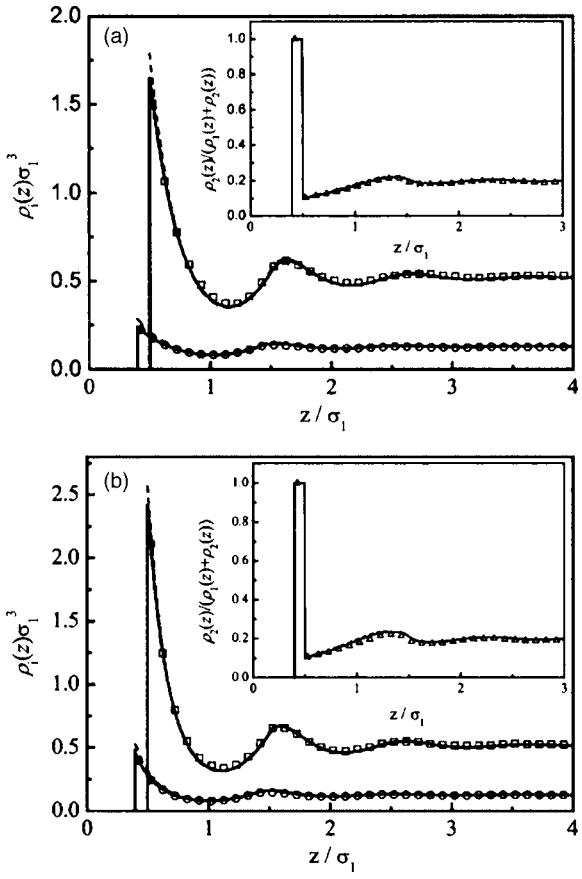

FIG. 5. Same as in Fig. 1 but at the diameter ratio $\sigma_2/\sigma_1=0.8$, reduced temperature $T^*=4.0$, energy parameter ratio $\varepsilon_2/\varepsilon_1=2.0$, bulk mole fraction $x_1^b=0.8$, and reduced density $\rho_b\sigma_1^3=0.65$.

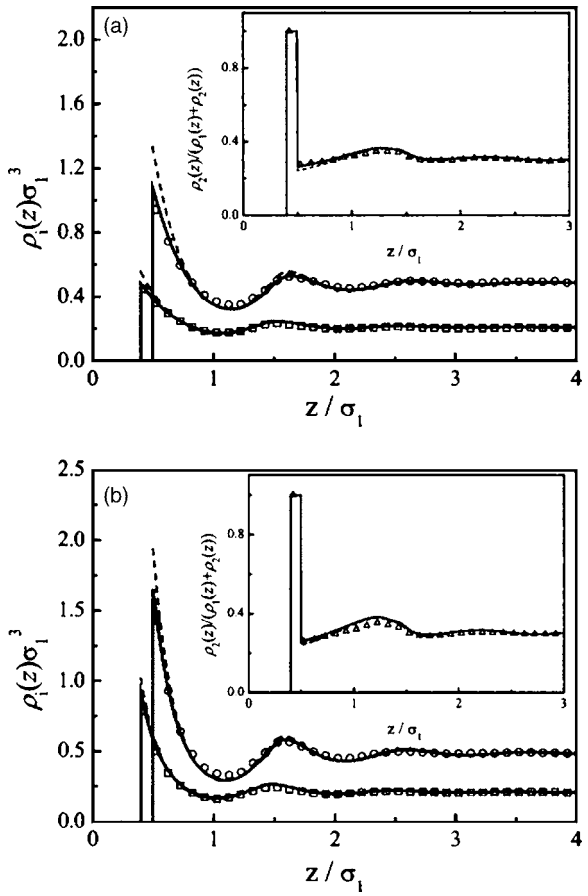

FIG. 6. Same as in Fig. 1 but at the diameter ratio $\sigma_2/\sigma_1=0.8$, reduced temperature $T^*=2.0$, energy parameter ratio $\varepsilon_2/\varepsilon_1=0.7$, bulk mole fraction $x_1^b=0.7$, and reduced density $\rho_b\sigma_1^3=0.7$.

MFMT-MF theory also behaves well at low bulk density, except for its slight overestimation of the density profile of the dominant component.

In Figs. 2–4, the density and local mole fraction profiles predicted from the density-functional theories are compared with those from the GCMC simulations carried out in this work at the reduced temperature $T^*=3.0$, diameter ratio $\sigma_2/\sigma_1=0.7$, reduced bulk density $\rho_b\sigma_1^3=0.6$, and different energy parameter ratios and bulk mole fractions. For these cases, the MFMT-*c*MF theory provides accurate contact values of density for each component, but the first valleys on the density profiles predicted by the MFMT-*c*MF theory are slightly deeper than that from the GCMC simulations. As expected, the MFMT-MF theory overestimates the density profiles for each component in the vicinity of the wall. However, the MFMT-MF predicts almost the same or slightly better local mole fraction profiles than the MFMT-*c*MF theory does. In general, both theories yield good local mole fraction profiles.

For higher bulk densities, the oscillations of the density profiles become more pronounced, as can be seen from Figs. 5–7. For the density profiles, similar results as in Figs. 1–4 can be found, but for the local mole fraction profile, the MFMT-*c*MF theory behaves better than the MFMT-MF theory does. It can be seen from Figs. 1–7 that the higher the wall energy parameter ε_w is, the larger is the magnitude of density oscillations. There is a significant accumulation of both component near the wall at high density and large value of ε_w. In all the cases presented in Figs. 1–7, surface segregation is observed and well described by both MFMT-*c*MF and MFMT-MF theories.

For the reduced density $\rho_b\sigma_1^3=0.6$ and reduced temperature $T^*=1.5$, the depletion of binary HCY fluids near a hard wall is observed in Fig. 8. This is the result of the competition between excluded-volume and attractive interactions. At low temperature, the attractive interaction prevails and the density profiles show depletion. The comparison of the DFT results with the GCMC simulation data shows that the MFMT-*c*MF theory gives excellent density and local mole fraction profiles in this case. Figure 8 demonstrates that the MFMT-MF theory is not only quantitatively unreliable but also qualitatively questionable due to its failure to describe the depletion near the wall. It can be concluded from Figs. 1–8 that at the reduced density, the wall energy parameter ε_W and the temperature increase and the oscillations of the density profiles become more pronounced, but those of the local mole fraction profiles have no apparent change. At low temperature, the depletion of binary HCY fluids near a hard wall can be observed.

B. Radial distribution function of binary HCY fluid mixtures

Based on the idea of Percus' test-particle method, the DFT can be used to calculate the radial distribution functions

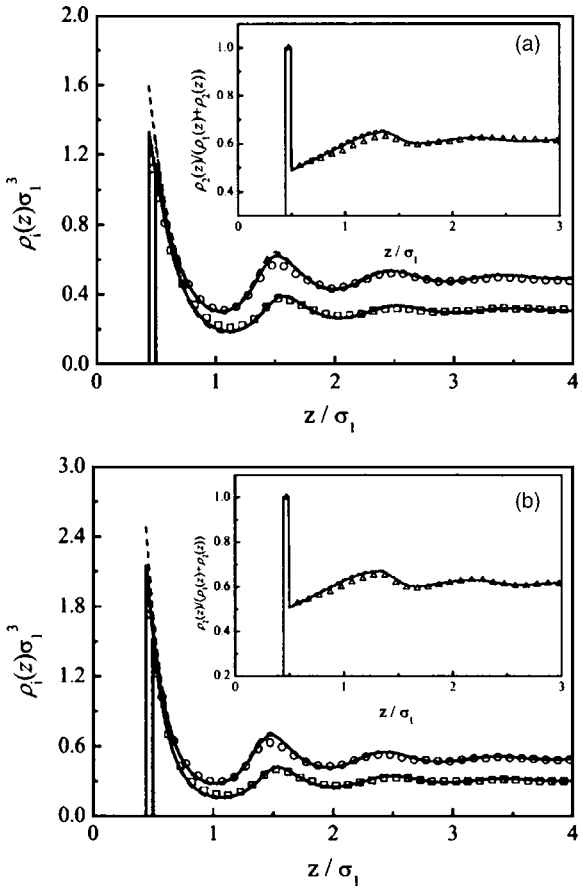

FIG. 7. Same as in Fig. 1 but at the diameter ratio $\sigma_2/\sigma_1=0.9$, reduced temperature $T^*=2.5$, energy parameter ratio $\varepsilon_2/\varepsilon_1=1.2$, bulk mole fraction $x_1^b=0.4$, and reduced density $\rho_b\sigma_1^3=0.8$.

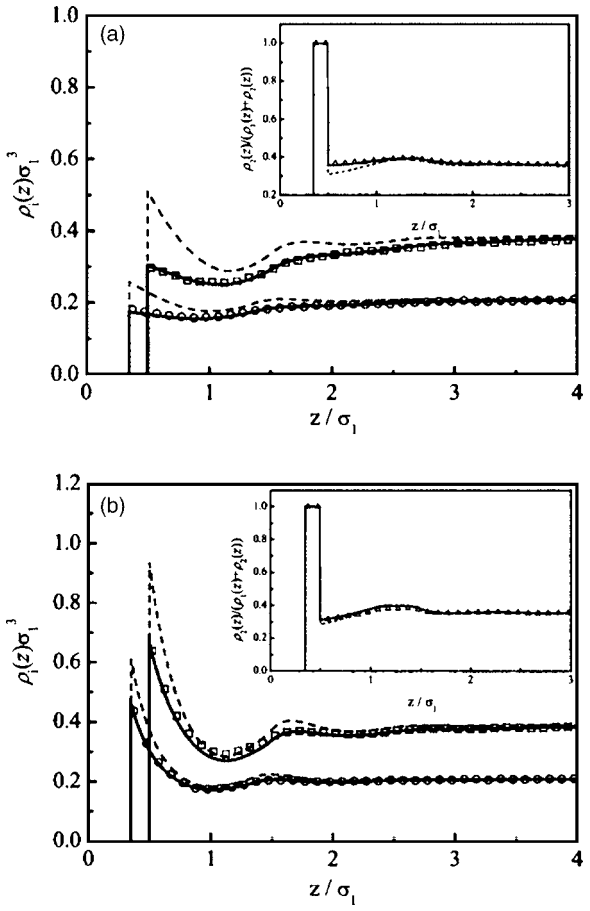

FIG. 8. Same as in Fig. 1 but at the diameter ratio $\sigma_2/\sigma_1=0.7$, reduced temperature $T^*=1.5$, energy parameter ratio $\varepsilon_2/\varepsilon_1=0.9$, bulk mole fraction $x_1^b=0.9$, and reduced density $\rho_b\sigma_1^3=0.6$.

of the bulk binary HCY fluid mixture. If we fix a Yukawa sphere, then the external potential produced by the fixed sphere is given by

$$V_i^{\text{ext}}(r)=\begin{cases}\infty, & r<\sigma_{ij}\\ -\dfrac{\varepsilon_{ij}\sigma_{ij}\exp[-\lambda(r/\sigma_{ij}-1)]}{r}, & r\geqslant\sigma_{ij}.\end{cases} \tag{19}$$

If the density profile of other spheres around the fixed particle is calculated from the DFT, the radial distribution function $g_{ij}(r)$ can be obtained through

$$g_{ij}(r)=\rho_i(r)/\rho_j^b. \tag{20}$$

Equation (20) has been applied to binary HCY fluid mixtures. Figures 9 and 10 depict the predicted radial distribution functions for the binary HCY fluid mixture at $T^*=3.0$, $\sigma_2/\sigma_1=0.7$, $\varepsilon_2/\varepsilon_1=0.5$, $x_1^b=0.65$, and $\rho_b\sigma_1^3=0.6$ and at $T^*=2.5$, $\sigma_2/\sigma_1=0.9$, $\varepsilon_2/\varepsilon_1=1.2$, $x_1^b=0.4$, and $\rho_b\sigma_1^3=0.8$, respectively, along with the Monte Carlo simulation results of this work. The results from both MFMT-*c*MF and MFMT-MF theories are in excellent agreement with those from the GCMC simulations. The contact values of the radial distribution functions from the FMT-*c*MF theory are very accurate for the considered binary mixture. Besides, from Figs. 9 and 10 we find that the radial distribution functions from the Percus' test-particle method are somewhat insensitive to the DFT used.

It should be pointed out that there is an alternative way to calculate the radial distribution functions via the second-order direct correlation functions obtained from the functional derivatives of the excess Helmholtz free-energy functional, i.e.,

$$\Delta C_{ij}^{(2)}(|\mathbf{r}'-\mathbf{r}|)=-\beta\frac{\delta^2F^{\text{ex}}[\{\rho_i(\mathbf{r})\}]}{\delta\rho_i(\mathbf{r})\,\delta\rho_j(\mathbf{r}')}. \tag{21}$$

The total correlation functions $h_{ij}(r)=g_{ij}(r)-1$ are calculated from the Ornstein-Zernike equation via the Fourier transform. Apparently, the more computational effort should be made, and less accurate radial distribution functions are obtained when compared to the Percus' test-particle method. Therefore only the latter method is used in this work.

C. Surface excess in slitlike pore

Given the density profiles for each component, the surface excess for component i in a slitlike pore is calculated as

$$\Gamma_i^{\text{ex}}=2\int_{\sigma_i/2}^{H/2}(\rho_i(z)-\rho_i^b)dz. \tag{22}$$

In Figs. 11 and 12, we compare the calculated surface excess with those from the GCMC simulations for binary HCY fluid mixtures in a slitlike pore at reduced temperature

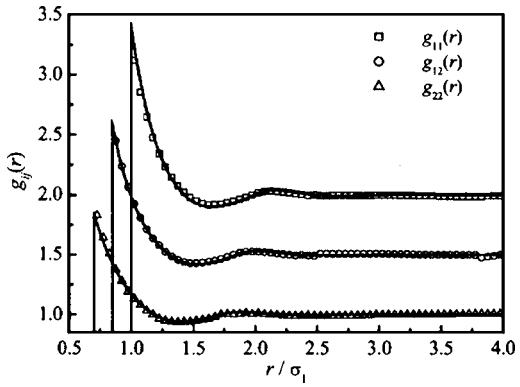

FIG. 9. Radial distribution functions of a binary HCY mixture at the diameter ratio $\sigma_2/\sigma_1=0.7$, reduced temperature $T^*=3.0$, energy parameter ratio $\varepsilon_2/\varepsilon_1=0.5$, bulk mole fraction $x_1^b=0.65$, and reduced density $\rho_b\sigma_1^3=0.6$. The symbols, dashed curves, and solid curves represent the results from the GCMC simulations, MFMT-MF, and MFMT-*c*MF theories, respectively. To enhance visual clarity, the RDFs of $g_{12}(r)$ and $g_{11}(r)$ are shifted upward by 0.5 and 1.0, respectively.

$T^*=3.0$, diameter ratio $\sigma_2/\sigma_1=0.7$, energy parameter ratio $\varepsilon_2/\varepsilon_1=0.5$, bulk mole fraction $x_1^b=0.5$, and wall energy parameters $\varepsilon_W/k_BT=0$ and 1.0.

For the hard wall without an attractive force, the surface excess of component 1 increases monotonically with the bulk density, while for the smaller one the surface excess first decreases with the bulk density (due to the depletion effect as shown in Fig. 8), exhibits a minimum, and finally rises as the density is further increased. The desorption to adsorption transition of attractive HCY mixture can be explained by the competition between the excluded volume and the attraction: the excluded volume favors the accumulation of fluid near the wall, but the attractions between Yukawa spheres are restricted close to the wall. Because the hard-sphere diameter of component 1 is larger, the excluded-volume effect is dominant and this leads to an accumulation in the pore. For the smaller molecule at low densities, the attraction between Yukawa spheres prevails and the density

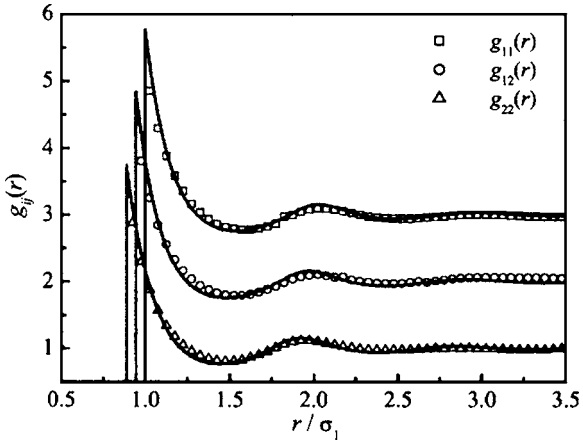

FIG. 10. Radial distribution functions of a binary Yukawa fluid mixture at the diameter ratio $\sigma_2/\sigma_1=0.9$, reduced temperature $T^*=2.5$, energy parameter $\varepsilon_2/\varepsilon_1=1.2$, bulk mole fraction $x_1=0.4$, and reduced density $\rho_b\sigma_1^3=0.8$. The symbols, dashed curves, and solid curves represent the results from the GCMC simulations, MFMT-MF, and MFMT-*c*MF theories, respectively. To enhance visual clarity, the RDFs of $g_{12}(r)$ and $g_{11}(r)$ are shifted upward by 1.0 and 2.0, respectively.

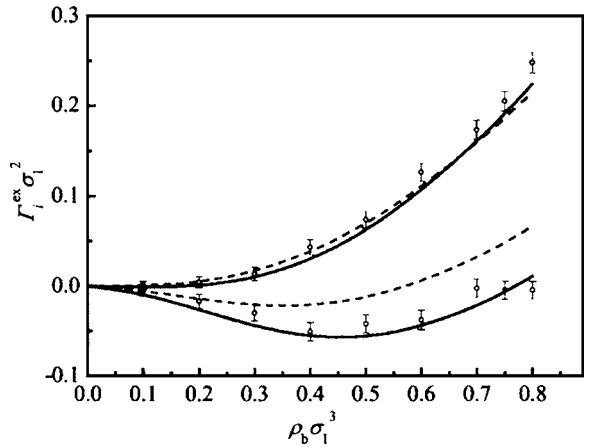

FIG. 11. Adsorption isotherms of a binary HCY mixture confined in a slitlike pore at the reduced temperature $T^*=3.0$, diameter ratio $\sigma_2/\sigma_1=0.7$, energy parameter ratio $\varepsilon_2/\varepsilon_1=0.5$, bulk mole fraction $x_1^b=0.5$, and energy parameter of wall $\varepsilon_W/k_BT=0$. The symbols, dashed curves, and solid curves represent the results from the GCMC simulation, MFMT-MF, and MFMT -*c*MF theories, respectively. The bars of symbols represent the statistical errors of the GCMC simulations.

profile shows depletion, leading to desorption. As the density increases, the density profiles are dominated by the excluded-volume effect and adsorption is observed. The MFMT-*c*MF theory correctly describes the adsorption of the larger molecule and the transition from desorption to adsorption for the smaller one, while the MFMT-MF theory substantially overestimates the surface excess of component 2. However, in the case of attractive walls, the MFMT-MF theory seems to give better results than the MFMT-*c*MF theory does due to the cancellation of overestimated density in the vicinity of the wall and the underestimated density at the first valley of the profiles. Comparing Fig. 11 with Fig. 12, one can see that the surface excess increases substantially with the increase of the wall energy parameter ε_W.

V. CONCLUSIONS

We have applied the grand canonical ensemble Monte Carlo simulation and the density-functional theory (DFT) to investigate the structures and adsorptions of the attractive hard-core Yukawa mixtures in a slitlike pore as well as the

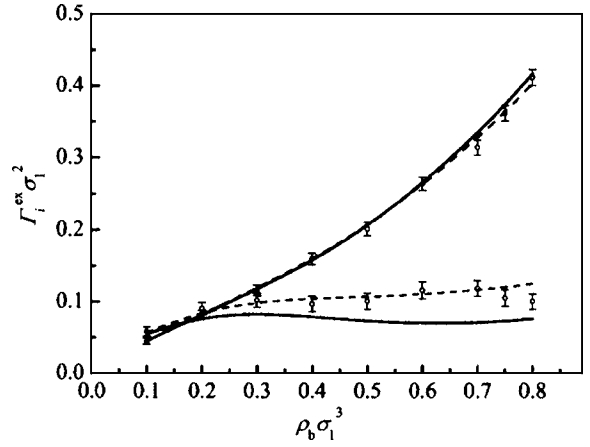

FIG. 12. Same as in Fig. 11 but for the energy parameter of wall $\varepsilon_W/k_BT=1.0$.

radial distribution functions of the bulk hard-core Yukawa mixtures. The DFT is based on the combination of the modified fundamental measure theory (MFMT) for the inhomogeneous hard-sphere contribution with the mean-field approximation (MF) of the Yukawa attractions. To cover the shortage of the overestimation of contact density at a wall, a correction parameter c is introduced to the MF approximation (cMF), just as we make a correction of the energy parameter in the well-known van der Waals equation of states. We found that parameter c with a value of 1.31 gives a satisfactory chemical potential for the pure attractive hard-core Yukawa fluids with $\lambda=1.8$ at reduced density $\rho_b\sigma^3=0.6$. Extensive comparisons of the predictions from DFT with the GCMC simulation results for the density and local mole fraction profiles indicate that the results of the MFMT-cMF theory has a significant improvement for density profiles and radial distribution functions over that of MFMT-MF theory, but little improvement is found for local mole fraction profiles. For the attractive hard-core Yukawa mixtures, there is a depletion near a hard wall at low temperature.

Both results of the GCMC simulations and the present MFMT-cMF theory have confirmed that the excluded-volume effect and the attraction between molecules have a significant effect on the adsorption/desorption of Yukawa fluids near a hard wall. The MFMT-cMF theory gives a better surface excess than the MFMT-MF theory does in a hard slitlike pore. For the binary Yukawa mixtures confined in the attractive slitlike pore, the MFMT-cMF theory gives an accurate surface excess of the larger molecule while it underestimates the surface excess of the smaller one.

We only make a simple correction of the MF theory regarding the correction parameter c as a constant, and the improvement of density profiles and adsorption isotherms for the binary hard-core Yukawa mixtures near a hard wall is obvious, while for the attractive wall, a further modification of the MF theory is required. The present MFMF-MF theory and its corrected form—MFMT-cMF theory—are simple in form, computationally efficient, and can be directly extended to the multicomponent and polydisperse hard-core Yukawa systems. Therefore, the method used in this work is very promising for practical applications such as multicomponent and polydisperse colloidal suspensions in confining geometry, inhomogeneous polydisperse dense plasmas, etc.

ACKNOWLEDGMENTS

This work is sponsored by the National Natural Science Foundation of China under Grant No. 20376037 and the National Basic Research Program of China under Grant No. 2003CB615700.

[1] S. M. Yang, H. Miguez, and G. A. Ozin, Adv. Funct. Mater. **12**, 425 (2002).
[2] D. Fu, Z.-C. Li, Y.-G. Li, and J.-F. Lu, Acta Chim. Sin. **61**, 1561 (2003).
[3] P. Gonzalez-Mozuelos, J. Alejandre, and M. Medina-Noyola, J. Chem. Phys. **95**, 8337 (1991).
[4] D. Fu and Y. Zhao, Acta Chim. Sin. **63**, 11 (2005).
[5] L. M. Sese and L. E. Bailey, J. Chem. Phys. **119**, 10256 (2003).
[6] T. W. Cochran and Y. C. Chiew, J. Chem. Phys. **121**, 1480 (2004).
[7] D. Fu, Y. Zhao, and Y.-G. Li, Ind. Eng. Chem. Res. **43**, 5425 (2004).
[8] K. P. Shukla, J. Chem. Phys. **112**, 10358 (2000).
[9] M. Gonzalez-Melchor, A. Trokhymchuk, and J. Alejandre, J. Chem. Phys. **115**, 3862 (2001).
[10] D.-M. Duh and L. Mier-Y-Teran, Mol. Phys. **90**, 373 (1997).
[11] D. Henderson, L. Blum, and J. P. Nowortya, J. Chem. Phys. **102**, 4973 (1995).
[12] D. Fu, Chin. J. Chem. Eng. **12**, 463 (2004).
[13] J. N. Herrera, L. Blum, and E. Garcia-Llanos, J. Chem. Phys. **105**, 9288 (1996).
[14] O. Vazquez, J. N. Herrera, and L. Blum, Physica A **325**, 319 (2003).
[15] W. Olivares-Rivas, L. Degreve, D. Henderson, and J. Quintana, J. Chem. Phys. **106**, 8160 (1997).
[16] J.-H. Yi and S.-C. Kim, J. Chem. Phys. **107**, 8147 (1997).
[17] Y. P. Tang and J. Z. Wu, Phys. Rev. E **70**, 011201 (2004).
[18] Y. P. Tang, J. Chem. Phys. **121**, 10605 (2004).
[19] F.-Q. You, Y.-X. Yu, and G.-H. Gao, J. Phys. Chem. B **109**, 3512 (2005).
[20] Y.-X. Yu and J. Z. Wu, J. Chem. Phys. **117**, 10156 (2002).
[21] Y.-X. Yu, J. Z. Wu, Y.-X. Xin, and G.-H. Gao, J. Chem. Phys. **121**, 1535 (2004).
[22] R. Roth, R. Evans, A. Lang, and G. Kahl, J. Phys.: Condens. Matter **14**, 12063 (2002).
[23] Y. Rosenfeld, J. Chem. Phys. **98**, 8126 (1993).
[24] D. Henderson, G. Stell, and E. Waisman, J. Chem. Phys. **62**, 4247 (1975).
[25] G. Stell and S. F. Sun, J. Chem. Phys. **63**, 5333 (1975).
[26] Y. P. Tang, J. Chem. Phys. **118**, 4140 (2003).
[27] R. Evans, in *Fundamentals of Inhomogeneous Fluids*, edited by D. Henderson (Marcel Dekker, New York, 1992).
[28] O. Pizio, A. Patrykiejew, and S. Sokolowski, J. Chem. Phys. **121**, 11957 (2004).
[29] C. Gu, G.-H. Gao, and Y.-X. Yu, J. Chem. Phys. **119**, 488 (2003).
[30] X. R. Zhang, D. P. Cao, and W. C. Wang, J. Chem. Phys. **119**, 12586 (2003).
[31] G. Wilemski and J. S. Li, J. Chem. Phys. **121**, 7821 (2004).
[32] B. Q. Lu, R. Evans, and M. M. Telo da Gama, Mol. Phys. **55**, 1319 (1985).
[33] E. Velasco and P. Tarazona, J. Chem. Phys. **91**, 7916 (1989).
[34] K. Katsov and J. D. Weeks, J. Phys. Chem. B **105**, 6738 (2001).
[35] K. Katsov and J. D. Weeks, J. Phys. Chem. B **106**, 8429 (2002).
[36] D. M. Huang and D. Chandler, J. Phys. Chem. B **106**, 2047 (2002).
[37] Y.-X. Yu and J. Z. Wu, J. Chem. Phys. **119**, 2288 (2003).
[38] Y. Rosenfeld, Phys. Rev. Lett. **63**, 980 (1989).
[39] T. Boublik, J. Chem. Phys. **53**, 471 (1970).
[40] G. A. Mansoori, N. F. Carnahan, K. E. Starling, and T. W. J. Leland, J. Chem. Phys. **54**, 1523 (1971).
[41] Y.-X. Yu, J. Z. Wu, and G.-H. Gao, J. Chem. Phys. **120**, 7223 (2004).
[42] C. N. Patra and S. K. Ghosh, J. Chem. Phys. **117**, 8938 (2002).
[43] D. Boda, W. R. Fawcett, D. Henderson, and S. Sokolowski, J. Chem. Phys. **116**, 7170 (2002).
[44] Y.-X. Yu, J. Z. Wu, and G.-H. Gao, Chin. J. Chem. Eng. **12**, 688 (2004).
[45] M. P. Allen and D. J. Tildesley, *Computer Simulation of Liquids* (Clarendon, Oxford, 1989).